Exact Relativistic Kinetic Theory of an Electron-Beam–Plasma System: Hierarchy of the Competing Modes in the System-Parameter Space

A. Bret,[1,2,*] L. Gremillet,[3,†] D. Bénisti,[3] and E. Lefebvre[3]

[1]*ETSI Industriales, Universidad de Castilla-La Mancha, 13071 Ciudad Real, Spain*

[2]*Instituto de Investigaciones Energéticas y Aplicaciones Industriales, Campus Universitario de Ciudad Real, 13071 Ciudad Real, Spain*

[3]*Département de Physique Théorique et Appliquée, CEA/DIF Bruyères-le-Châtel, 91297 Arpajon Cedex, France*

(Received 7 December 2007; published 23 May 2008)

The stability analysis of an electron-beam–plasma system is of critical relevance in many areas of physics. Surprisingly, decades of extensive investigation have not yet resulted in a realistic unified picture of the multidimensional unstable spectrum within a fully relativistic and kinetic framework. All attempts made so far in this direction were indeed restricted to simplistic distribution functions and/or did not aim at a complete mapping of the beam-plasma parameter space. The present Letter comprehensively tackles this problem by implementing an exact linear model. Three kinds of modes compete in the linear phase, which can be classified according to the direction of their wave number with respect to the beam. We determine their respective domain of preponderance in a three-dimensional parameter space and support our results with multidimensional particle-in-cell simulations.

DOI: 10.1103/PhysRevLett.100.205008 PACS numbers: 52.40.Mj, 52.35.Qz, 52.57.Kk

Relativistic electron beams moving through a collisionless background plasma are ubiquitous in a variety of physical systems pertaining, e.g., to inertial confinement fusion [1], the solar corona [2], electronic pulsar winds [3], accreting black hole systems [4], active galactic nuclei [5], or γ-ray burst sources [6]. Regardless of its setting, the electron-beam–plasma system has been known to be prone to collective processes since the very early studies on the so-called two-stream instability [7], which is of electrostatic nature and therefore characterized by wave and electric field vectors both parallel to the beam flow direction. Later on, another class of unstable modes was discovered: usually referred to as ''filamentation'' [8] or Weibel modes [9], they are mostly electromagnetic, purely growing, and develop preferentially in the plane normal to the beam. Finally, unstable modes propagating obliquely to the beam were investigated [10] and found to rule the system in case of cold and diluted relativistic electron beams [11–13]. To date, the few kinetic approaches investigating the whole two-dimensional (2D) unstable spectrum have been restricted to nonrelativistic energy spreads [14] or to waterbaglike distribution functions of questionable validity at high energy spreads [15]. Among the salient features of the oblique modes revealed by the latter studies are their mostly electrostatic character and usually efficient interaction with both the beam and plasma components. Yet, because of various limitations, all the models considered so far have failed to provide a complete picture of the hierarchy of the competing unstable modes as a function of the system parameters. One should stress that addressing this long-standing issue, which is the main goal of the present Letter, is a critical prerequisite to understanding the nonlinear aspects of the beam-plasma interaction. Among these are the instability-induced collective stopping and scattering, whose level is expected to depend closely on the nature (i.e., electrostatic or electromagnetic) of the underlying processes [16–24].

In contrast to past studies, the fully relativistic kinetic model implemented here involves, for both the counterstreaming beam and plasma populations (hereafter identified by the subscripts b and p), unperturbed distribution functions in the form of drifting Maxwell-Jüttner functions [25–27]

$$f_\alpha^0(\mathbf{p}) = \frac{\mu_\alpha}{4\pi\gamma_\alpha^2 K_2(\mu_\alpha/\gamma_\alpha)} \exp[-\mu_\alpha(\gamma(\mathbf{p}) - \beta_\alpha p_y)], \tag{1}$$

which allow for arbitrary energy spreads and drifts. Here $\alpha = (b, p)$ stands for the beam or plasma component, $\beta_\alpha = \langle p_y/\gamma \rangle$ is the normalized y-aligned mean drift velocity, γ_α the corresponding relativistic factor, and $\mu_\alpha = mc^2/k_B T_\alpha$ the normalized inverse temperature of each electron component. All momenta are normalized by mc. K_2 denotes a modified Bessel function of the second kind. Current neutralization is assumed, that is, $n_b\beta_b + n_p\beta_p = 0$, where n_b and n_p are the beam and plasma mean densities, respectively. From now on, the ions form a fixed neutralizing background and collisions are neglected. It is noteworthy that the above model distribution function is provided a thermodynamically consistent derivation from first principles in Ref. [25,26], where it is shown to maximize the specific entropy for fixed values of each species' total momentum and energy. In addition to its thermodynamic grounds, this distribution function is helpful in gaining insight into the stability properties of *smooth* relativistic distributions, as opposed to the commonly used waterbag distributions [28–30], severely flawed by the neglect of Landau damping. The evolution of the initially homogeneous and unmagnetized system is governed by the relativistic Vlasov-Maxwell set of equations. Following a

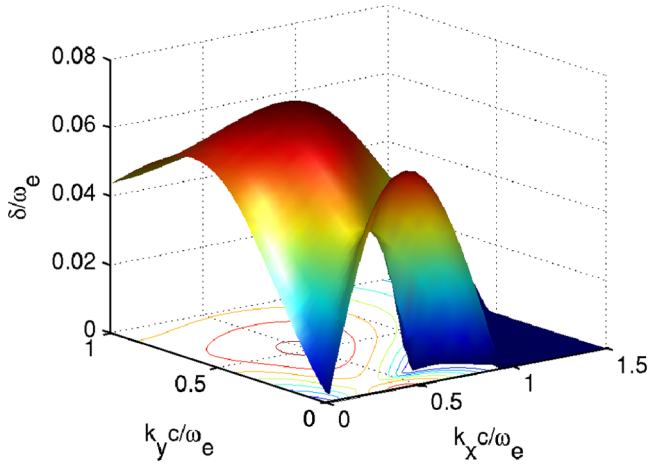

FIG. 1 (color online). Normalized growth rate in the (k_x, k_y) plane for $n_b/n_p = 1$, $\gamma_b = 1.2$, $T_b = 500$ keV and $T_p = 5$ keV. Isocontours are linearly spaced from 0.01 to 0.07.

routine procedure, the general dispersion equation for any orientation of the wave vector is derived [30,31] and solved numerically. Details of the numerical procedure will be presented elsewhere. Introducing the total electron plasma frequency ω_e, and normalizing the complex frequency ω and wave vector $\mathbf{k}$ by ω_e and ω_e/c, respectively, there remain four independent variables: the beam mean relativistic factor γ_b, the beam and plasma temperatures T_b and T_p, and the density ratio n_b/n_p. A typical map of the growth rate $\delta = \Im\omega$ is displayed in Fig. 1 for $n_b/n_p = 1$, $\gamma_b = 1.2$, $T_b = 500$ keV, and $T_p = 5$ keV. The three aforementioned instability classes are clearly visible for this configuration. For wave vectors aligned with the beam, the two-stream instability peaks for $k_y \sim 0.5$ whereas, in the perpendicular direction, the fastest growing filamentation mode is found for $k_x \sim 0.5$. Overall, though, the 2D unstable spectrum is here dominated by an oblique mode located at $(k_x, k_y) \sim (0.5, 0.5)$.

The three instability classes do not share the same sensitivity to the beam temperature, drift, and density. This yields a nontrivial dependence of the growth rates on the system parameters, hence a varying hierarchy between the instability classes. Assuming from now on a fixed plasma temperature $T_p = 5$ keV, it is possible to determine the regions of predominance of each instability class in the $(n_b/n_p, \gamma_b, T_b)$ space. The surfaces that delimit regions governed by different instability classes are displayed in Fig. 2(a) and shaded according to the local maximum growth rate. Points located between the plane $\gamma_b = 1$ and the left surface define systems dominated by the two-stream instability, while those located between the right surface and the plane $n_b/n_p = 1$ pertain to filamentation-ruled systems. Oblique modes prove to govern the rest of the parameter space.

The two-stream instability is seen to prevail in the whole nonrelativistic range of the beam drift energy ($\gamma_b - 1 \ll 1$), as well as in weakly relativistic systems with hot enough beams. The reason for the latter feature is as follows: first, filamentation is strongly weakened for weakly energetic beams because its growth rate is proportional to the beam velocity. Being thus left with the two-stream and oblique modes, we note that the former are handicapped by the relativistic increase in the longitudinal inertia, while the latter are more sensitive to the beam temperature. As a consequence of these effects, a system characterized by $n_b/n_p = 0.1$, $\gamma_b = 1.5$, and $T_b = 500$ keV turns out to be mostly subject to the two-stream

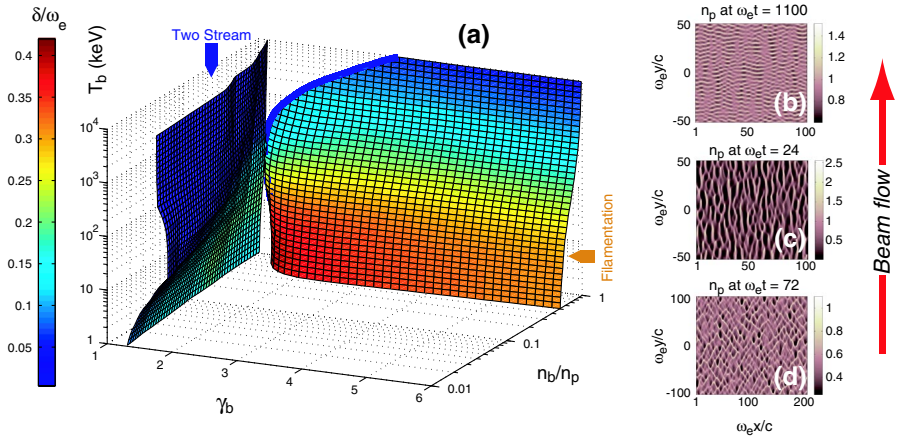

FIG. 2 (color online). Left: Hierarchy of the unstable modes in the $(n_b/n_p, \gamma_b, T_b)$ parameter space for $T_p = 5$ keV. The left surface delimits the two-stream-dominated domain (at low γ_b) and the oblique-mode-dominated domain, whereas the right surface delimits the filamentation-dominated domain (at high n_b/n_p) and the oblique-mode-dominated domain. Right: Plasma density profiles at the end of the linear phase as predicted by 2D PIC simulations run with three different sets of parameters: $n_b/n_p = 0.1$, $\gamma_b = 1.5$, and $T_b = 500$ keV (b); $n_b/n_p = 1$, $\gamma_b = 1.5$, and $T_b = 100$ keV (c); $n_b/n_p = 1$, $\gamma_b = 1.5$, and $T_b = 2$ MeV (d). In all cases, $T_p = 5$ keV. In agreement with linear theory, the three resulting patterns evidence regimes dominated by two-stream, filamentation, and oblique modes, respectively.

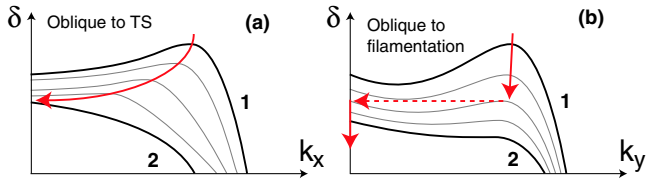

FIG. 3 (color online). Typical evolution of the fastest growing mode (arrow) for the oblique to two-stream (a) and oblique to filamentation (b) transitions, of which only the former is continuous.

instability, as indicated in Fig. 2(a). We have checked this prediction by means of a 2D particle-in cell (PIC) simulation using the massively parallel code CALDER [32]. As expected, the plasma density profile, displayed in Fig. 2(b) at the time when the instability starts to saturate, exhibits modulations preferentially along the drift direction. By repeating the Fourier analysis performed in Ref. [15], we have verified that the simulated **k**-resolved growth rates closely agree with linear theory.

Let us now consider the filamentation-to-oblique transition, which is found to take place for dense and relativistic beams. The shape of the corresponding frontier is here more involved than the previous one as it stems from a balance between the three system parameters. The filamentation growth rate increases with the beam density and decreases with temperature more rapidly than the oblique mode growth rate. For a cold system [13], this growth rate scales like $\beta_b/\sqrt{\gamma_b}$, which reaches a maximum for $\gamma_b = \sqrt{3}$. Still in the cold limit, the filamentation-to-oblique frontier reaches a minimum $n_b/n_p \sim 0.53$ for $\gamma_b \sim 3$. The resulting boundary proves to be mostly determined by γ_b for dense, cold, and weakly relativistic beams. In the relativistic and ultrarelativistic regimes, the main parameter is the beam density, although high enough beam temperatures always end up favoring oblique modes. This result goes against the conventional belief that relativistic systems with $n_b/n_p = 1$ are governed by filamentation [33,34]. We show here that this behavior holds true only as long as the beam is not too hot. This is illustrated in Fig. 2(c) and 2(d) which compares the simulated plasma density profiles for two values of the beam temperature, respectively, below and above the filamentation-to-oblique boundary. The other parameters are $n_b/n_p = 1$ and $\gamma_b = 1.5$. In accord with linear theory, filamentation modes are seen to prevail when $T_b = 100$ keV, whereas oblique modes clearly take over when $T_b = 2$ MeV, yielding a characteristic knittedlike pattern.

When crossing one of the transition surfaces displayed in Fig. 2(a), a phase velocity discontinuity may occur as regards the dominant mode. During the oblique to two-stream transition, the k_y component of the most unstable mode remains almost constant while the k_x component steadily decreases down to zero [Fig. 3(a), curve 2]. The oblique to two-stream transition is therefore continuous, notably as regards the resulting phase velocity change. During the oblique to filamentation transition [Fig. 3(b)], by contrast, the k_x component hardly varies, whereas the k_y component evolves as follows. Let us start from a system ruled by an oblique mode with $k_y \neq 0$ and $\Re\omega \neq 0$ [Fig. 3(b), curve 1]. As the system moves to the filamentation regime, the k_y component of the dominant mode remains almost constant while its growth rate gradually weakens. When the latter eventually becomes smaller than that of the main filamentation mode (with $k_y = \Re\omega = 0$), the system experiences a sudden change regarding its dominant wave phase velocity, which then switches from a finite value to zero.

So as to gain insight into the field generation within a more realistic geometry, we have performed a three-

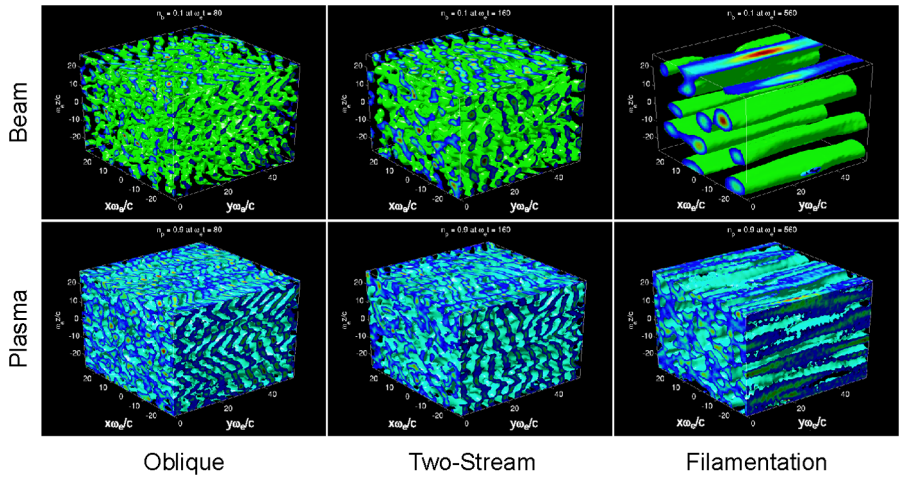

FIG. 4 (color online). 3D PIC simulation initialized with $n_b/n_p = 0.1$, $\gamma_b = 3$, $T_b = 50$ keV, and $T_p = 5$ keV: isosurfaces of the beam and plasma density profiles at $\omega_e t = 80$, 160, and 560. The system runs through three successive phases, each governed by a distinct instability class.

dimensional PIC simulation of a diluted beam-plasma system defined by $n_b/n_p = 0.1$, $\gamma_b = 3$, $T_b = 50$ keV, and $T_p = 5$ keV (Fig. 4). In agreement with Fig. 2(a), the system is initially governed by oblique modes, as confirmed by the beam and plasma profiles at $\omega_e t = 80$. Later on ($\omega_e t = 160$), though, the system gets ruled by two-stream modes. A rough, quasilinearlike argument supporting this transition can be given assuming that the beam distribution function has retained a Maxwell-Jüttner form. At $\omega_e t = 160$ the best fit is obtained for $\gamma_b \sim 1.6$ and $T_b \sim 200$ keV. Because of the low beam density, we can reasonably neglect the changes in the plasma distribution function. Figure 2(a) then indicates that the system is indeed dominated by two-stream modes. After saturation of all electrostatic modes, the system eventually reaches a filamentation regime, owing to a remaining, high enough anisotropy, as already observed in Ref. [15]. Yet, this transition cannot be explained in light of the present linear model because the distribution functions then strongly depart from the form (1).

Let us conclude by making two important remarks. First, given our model distribution function (1), complete linear stabilization of the system can never be achieved in the whole parameter space. In particular, the maximum filamentation growth rate can be shown to scale like $1/T_b^{3/2}$ in the large T_b limit. Second, the oblique/filamentation boundary in the plane $T_b = 1$ keV behaves like $n_b/n_p \sim 1 - 0.86\gamma_b^{-1/3}$ when $\gamma_b \gg 1$. As a result, the filamentation-ruled region is all the more squeezed against the plane $n_b/n_p = 1$ when the beam energy is high. This also implies that the ultrarelativistic regime is asymptotically oblique unless $n_b/n_p = 1$. This could bear important consequences in a number of astrophysical scenarios which involve relativistic factors up to 10^3 and beyond [35–37].

Thanks are due to Claude Deutsch and Marie-Christine Firpo for enriching discussions. This work has been partially achieved under Projects No. FIS 2006-05389 of the Spanish Ministerio de Educación y Ciencia, and No. PAI08-0182-3162 of the Consejería de Educación y Ciencia de la Junta de Comunidades de Castilla-La Mancha. The simulation work was performed using the computer facilities of CEA/CCRT.

*antoineclaude.bret@uclm.es
†laurent.gremillet@cea.fr

[1] M. Tabak, J. Hammer, M. E. Glinsky, W. L. Kruer, S. C. Wilks, J. Woodworth, E. M. Campbell, M. D. Perry, and R. J. Mason, Phys. Plasmas **1**, 1626 (1994).
[2] A. Klassen, M. Karlicky, and G. Mann, Astron. Astrophys. **410**, 307 (2003).
[3] L. Mestel, J. Astrophys. Astron. **16**, 119 (1995).
[4] R. Fender and T. Belloni, Annu. Rev. Astron. Astrophys. **42**, 317 (2004).
[5] J. A. Zensus, Annu. Rev. Astron. Astrophys. **35**, 607 (1997).
[6] T. Piran, Rev. Mod. Phys. **76**, 1143 (2005).
[7] D. Bohm and E. P. Gross, Phys. Rev. **75**, 1851 (1949); **75**, 1864 (1949).
[8] B. Fried, Phys. Fluids **2**, 337 (1959).
[9] E. S. Weibel, Phys. Rev. Lett. **2**, 83 (1959).
[10] S. A. Bludman, K. M. Watson, and M. N. Rosenbluth, Phys. Fluids **3**, 747 (1960).
[11] Y. B. Faĭnberg, V. D. Shapiro, and V. Shevchenko, Sov. Phys. JETP **30**, 528 (1970).
[12] F. Califano, R. Prandi, F. Pegoraro, and S. V. Bulanov, Phys. Rev. E **58**, 7837 (1998).
[13] A. Bret and C. Deutsch, Phys. Plasmas **12**, 082704 (2005).
[14] A. Bret, M.-C. Firpo, and C. Deutsch, Phys. Rev. Lett. **94**, 115002 (2005).
[15] L. Gremillet, D. Bénisti, E. Lefebvre, and A. Bret, Phys. Plasmas **14**, 040704 (2007).
[16] R. Davidson, C. Wagner, D. Hammer, and I. Haber, Phys. Fluids **15**, 317 (1972).
[17] L. Thode and R. Sudan, Phys. Fluids **18**, 1552 (1975).
[18] T. Okada and K. Niu, J. Plasma Phys. **23**, 423 (1980).
[19] M. Honda, J. Meyer-ter-Vehn, and A. Pukhov, Phys. Rev. Lett. **85**, 2128 (2000).
[20] M. Medvedev, M. Fiore, R. Fonseca, L. Silva, and W. Mori, Astrophys. J. **618**, L75 (2005).
[21] F. Califano, T. Cecchi, and C. Chiuderi, Phys. Plasmas **9**, 451 (2002).
[22] J. T. Mendonça, P. Norreys, R. Bingham, and J. R. Davies, Phys. Rev. Lett. **94**, 245002 (2005).
[23] J. C. Adam, A. Héron, and G. Laval, Phys. Rev. Lett. **97**, 205006 (2006).
[24] T. Okada and K. Ogawa, Phys. Plasmas **14**, 072702 (2007).
[25] F. Jüttner, Ann. Phys. (Leipzig) **339**, 856 (1911).
[26] P. Wright and G. Hadley, Phys. Rev. A **12**, 686 (1975).
[27] D. Cubero, J. Casado-Pascual, J. Dunkel, P. Talkner, and P. Hänggi, Phys. Rev. Lett. **99**, 170601 (2007).
[28] P. H. Yoon and R. C. Davidson, Phys. Rev. A **35**, 2718 (1987).
[29] L. O. Silva, R. A. Fonseca, J. W. Tonge, W. B. Mori, and J. M. Dawson, Phys. Plasmas **9**, 2458 (2002).
[30] A. Bret, M.-C. Firpo, and C. Deutsch, Phys. Rev. E **70**, 046401 (2004).
[31] S. Ichimaru, *Basic Principles of Plasma Physics* (W. A. Benjamin, Inc., Reading, Massachusetts, 1973).
[32] E. Lefebvre, N. Cochet, S. Fritzler, V. Malka, M.-M. Aleonard, J.-F. Chemin, S. Darbon, L. Disdier, J. Faure, and A. Fedotoff *et al.*, Nucl. Fusion **43**, 629 (2003).
[33] J. Wiersma and A. Achterberg, Astron. Astrophys. **428**, 365 (2004).
[34] F. Califano, D. D. Sarto, and F. Pegoraro, Phys. Rev. Lett. **96**, 105008 (2006).
[35] M. Dieckmann, Phys. Rev. Lett. **94**, 155001 (2005).
[36] F. Aharonian, A. Belyanin, E. Derishev, V. Kocharovsky, and V. Kocharovsky, Phys. Rev. D **66**, 023005 (2002).
[37] M. Medvedev and A. Loeb, Astrophys. J. **526**, 697 (1999).